



HAL
open science

Biological physics by high-speed atomic force microscopy

Ignacio Casuso, Lorena Redondo-Morata, Felix Rico

► **To cite this version:**

Ignacio Casuso, Lorena Redondo-Morata, Felix Rico. Biological physics by high-speed atomic force microscopy. *Philosophical Transactions of the Royal Society A: Mathematical, Physical and Engineering Sciences*, 2020, 378 (2186), pp.20190604. 10.1098/rsta.2019.0604 . hal-03027169

HAL Id: hal-03027169

<https://hal.science/hal-03027169>

Submitted on 27 Nov 2020

HAL is a multi-disciplinary open access archive for the deposit and dissemination of scientific research documents, whether they are published or not. The documents may come from teaching and research institutions in France or abroad, or from public or private research centers.

L'archive ouverte pluridisciplinaire **HAL**, est destinée au dépôt et à la diffusion de documents scientifiques de niveau recherche, publiés ou non, émanant des établissements d'enseignement et de recherche français ou étrangers, des laboratoires publics ou privés.

Journal: **PHILOSOPHICAL TRANSACTIONS OF THE ROYAL SOCIETY A**

Article id: **RSTA20190604**

Article Title: **Biological physics by high-speed atomic force microscopy**

First Author: Ignacio Casuso

Corr. Author(s): Felix Rico


AUTHOR QUERIES – TO BE ANSWERED BY THE CORRESPONDING AUTHOR

As the publishing schedule is strict, please note that this might be the only stage at which you are able to thoroughly review your paper.

Please pay special attention to author names, affiliations and contact details, and figures, tables and their captions.

No changes can be made after publication.

The following queries have arisen during the typesetting of your manuscript. Please answer these queries by marking the required corrections at the appropriate point in the text.

SQ1	Please confirm that this paper is intended to be Open Access. The charge for Open Access should be paid before publication. If you have not yet received an email requesting payment please let us know when returning your corrections. 
Q1	Please provide publisher location [city/state/country] details in reference [8].
Q2	Please supply the page range in reference [24].
Q3	References [26,43] (in the author file) have been repeated and hence the repeated version have been deleted and then renumbered. Please check.
Q4	Please supply the year of publication in references [28,60,68,71].
Q5	Please supply the page range in reference [123].

royalsocietypublishing.org/journal/rsta

Research



Cite this article: Casuso I, Redondo-Morata L, Rico F. 2020 Biological physics by high-speed atomic force microscopy. *Phil. Trans. R. Soc. A* 20190604.

<http://dx.doi.org/10.1098/rsta.2019.0604>

Accepted: 7 August 2020

One contribution of 9 to a discussion meeting issue 'Dynamic in-situ microscopy relating structure and function'.

Subject Areas:

biomechanics, biophysics, nanotechnology, statistical physics, cellular biophysics

Keywords:

high-speed force spectroscopy, single molecules, biophysics, membranes, proteins, cells

Author for correspondence:

Felix Rico

e-mail: felix.rico@inserm.fr

Biological physics by high-speed atomic force microscopy

Ignacio Casuso¹, Lorena Redondo-Morata² and Felix Rico¹

¹Aix-Marseille University, Inserm, CNRS, LAI, 163 Av. de Luminy, 13009 Marseille, France

²Center for Infection and Immunity of Lille, INSERM U1019, CNRS UMR 8204, 59000 Lille, France

IC, 0000-0001-7192-0136; FR, 0000-0002-7757-8340

While many fields have contributed to biological physics, nanotechnology offered a new scale of observation. High-speed atomic force microscopy (HS-AFM) provides nanometre structural information and dynamics with subsecond resolution of biological systems. Moreover, HS-AFM allows us to measure piconewton forces within microseconds giving access to unexplored, fast biophysical processes. Thus, HS-AFM provides a tool to nourish biological physics through the observation of emergent physical phenomena in biological systems. In this review, we present an overview of the contribution of HS-AFM, both in imaging and force spectroscopy modes, to the field of biological physics. We focus on examples in which HS-AFM observations on membrane remodelling, molecular motors or the unfolding of proteins have stimulated the development of novel theories or the emergence of new concepts. We finally provide expected applications and developments of HS-AFM that we believe will continue contributing to our understanding of nature, by serving to the dialog between biology and physics.

This article is part of the discussion meeting issue 'Dynamic *in situ* microscopy relating structure and function'.

© 2020 The Authors. Published by the Royal Society under the terms of the Creative Commons Attribution License <http://creativecommons.org/licenses/by/4.0/>, which permits unrestricted use, provided the original author and source are credited.

1. Introduction

The dialogue between physics and biology exists since the first experiments of Helmholtz on the mechanics of the eye and the discoveries by Galvani and Volta on electrical stimuli of frog muscles [1,2]. The dialog continued with the speculative analysis of Schrodinger and the discovery of the structure of DNA, evolving into a field in itself through the application of optical traps to biomolecules [3–7]. In the era of quantitative biology, application of new tools to obtain physical understanding of biology seem necessary. Moreover, as the most fundamental questions in physics reach a stalled point, turning the eyes into biological systems in search of emergent physical phenomena seems inevitable [8]. Biological physics involves studying biological systems from which physical concepts and principles emerge and stand independently of the original system [9–11]. Biological processes are subjected to thermal fluctuations at the nanoscale and provide a gigantic playground to explore emergence of physical phenomena. On the one hand, single-molecule optical microscopy techniques are particularly well suited to study the dynamics of molecules with excellent time resolution but are limited to labelled protein regions [12]. On the other hand, high-resolution techniques like X-ray crystallography and cryo-electron microscopy had important impact the field of structural molecular biology but they provide still images based on ensemble averaging [13]. The apparition of nanotools has boosted the field of biological physics at the nanoscale. The first experiments on single biomolecules opened the door towards physical understanding of biomolecules, the stepping mechanisms of molecular motors or the binding strength of receptor/ligand bonds [14–22]. Furthermore, nanotechnologies allowed direct verification of fundamental fluctuation–dissipation theorems on single biomolecules in a paradigmatic example of biological physics [5,23].

The atomic force microscope was since its invention in 1986 [24] quickly positioned among the single-molecule, high-resolution structural analysis techniques. Atomic force microscopy (AFM) is in its thirties and an established methodology among the biophysical community as a stand-alone, high-resolution imaging technique and force transducer [25]. AFM provides pN force sensitivity and nanometre resolution and allows thus mechanical measurements and high-resolution imaging in liquid, at ambient temperature and pressure, being optimal for biological applications. While the contribution AFM as an imaging tool to biological physics has been relatively limited, as a force tool AFM has been extensively useful. The major drawback of AFM is the relatively low temporal resolution, requiring minutes to obtain a single image and limiting force measurements to approximately 0.1 milliseconds. The development of ultrashort cantilevers with microsecond time resolution and fast electronics and piezoelectric scanners allowed reaching 1000-fold faster frame rates, which led to the emerge of what now is named high-speed AFM (HS-AFM). The development and application of HS-AFM imaging is introducing a new dimension to structural biology: time [26,27]. HS-AFM allows the visualization of conformational changes of proteins in real time. HS-AFM imaging has been used to study a number of biological systems, such as the activity of proton pumps, the dynamic interaction of proteins with DNA, ligand-induced conformational changes in ion channels, and the diffusion and assembly of membrane and scaffold proteins [28–33]. Moreover, the flexibility of biomolecules has also been reported on antibodies showing the capacity of this essential molecules to adapt their shape for better binding to the target [34]. Moreover, ultrashort HS-AFM cantilevers enables high-speed force spectroscopy (HS-FS) measurements with μ s time resolution to explore fast protein dynamics, challenge theoretical predictions and allow direct comparison with molecular dynamics (MD) simulations.

In this review, we tried to focus on contributions of HS-AFM on biological physics, i.e. on physical phenomena that occur in biological systems at the nanoscale. While the emergence of HS-AFM is relatively young, an exhaustive review of all published works would be enormous. Thus, the present review is not meant to be comprehensive and we already apologize for the missing works that could not fit here. The chosen HS-AFM works we report have been driven, unavoidably, by personal interest but also because they represent examples in which physics is central, leaving the biological system itself as secondary. Since some of the physical

concepts may not be familiar, we have tried to provide a short introduction to the topic. First, we briefly describe the main developments allowing HS-AFM. We then focus on applications of HS-AFM to biological systems and processes in which physics plays a major role: dynamic organization of membranes, molecular machines, dynamic (un)folding of proteins and single-molecule mechanics. The review includes both applications of HS-AFM imaging and HS-FS.

2. HS-AFM

The first time that the concept of high-speed AFM was mentioned -to our knowledge- was in 1991 by Barrett & Quate [35], who provided a fair attempt with the technology available at that time. The groups of Hansma and Ando would challenge the practical speed limitations [36,37]. In 2010, the Ando's group filmed individual myosin molecules walking on an actin filament [38], operating their HS-AFM instrument at a speed about 1000 times faster than conventional AFM systems. Besides the visual impact and scientific insight of those movies, these experiments illustrated that HS-AFM was able to obtain concomitantly structural and dynamic data of biomolecules, providing insights inaccessible to any other method.

(a) High-speed imaging and force spectroscopy

AFM modes that have an intermittent tip-sample contact are commonly used for the study of biological samples to minimize damage and mechanical perturbation. The most often intermittent contact-mode used is acoustic-modulation (tapping) mode, in which the AFM cantilever is excited at its resonance frequency. The resulting oscillating tip is intermittently contacting -tapping- the surface, which consequently damps the oscillation amplitude. The surface topography is reconstructed by monitoring the amplitude of the oscillating cantilever. While scanning in the x - y plane, the amplitude of the cantilever oscillation is kept constant thanks to a proportional-integral-derivative feedback controller that controls the z position. HS-AFM is nowadays almost exclusively operated in tapping-mode to minimize the force or amount of energy transferred at the tip-sample contact. The maximum rates of HS-AFM range between 5 and 20 frames per second (fps) [39]. While different approaches have been introduced to allow fast scanning rates [40,41], the miniaturization of the moving components of the AFM (cantilever and scanner) and faster electronics are the basis of the technical developments which allow reaction responses of microseconds and consequently to increase the imaging rate [42]. In brief, the most important elements that allow AFM to be operated at a video-rate are (figure 1):

- (1) *Ultras-small cantilevers*. Modern microfabrication techniques allow reducing the cantilever dimensions to $7\ \mu\text{m}$ long, $2\ \mu\text{m}$ wide and $90\ \text{nm}$ thick (considerably smaller than conventional cantilevers, $40\text{--}200\ \mu\text{m}$ long, $20\text{--}30\ \mu\text{m}$ wide and $400\text{--}800\ \text{nm}$ thick). This is probably the most critical point for HS-AFM imaging: the reduction of the cantilever mass allows achieving high resonance frequencies of approximately $500\ \text{kHz}$ in liquid and short response times (approx. $1\ \mu\text{s}$). Long amorphous carbon deposits are grown on the cantilever, which serve as a tip once etched.
- (2) *Fast actuators*. The z -piezo scanner is driven by high-frequency signals during high-speed imaging, that generate mechanical vibrations. To minimize the vibrations, a dummy piezo is placed in the opposite direction and actuated simultaneously in order to counterbalance the impulsive force. Furthermore, z -scanners are individually calibrated, and the resonance frequencies filtered out. The x - and y -piezo actuators -larger than the z -piezo- keep their centres of mass stationary using flexure stages and by attaching a balance weight to the counter side. They are also embedded in a silicon elastomer to passively damp vibrations.
- (3) *Fast amplitude detectors*. The cantilever oscillation amplitude is measured and output by a Fourier method at every cycle of the oscillation.

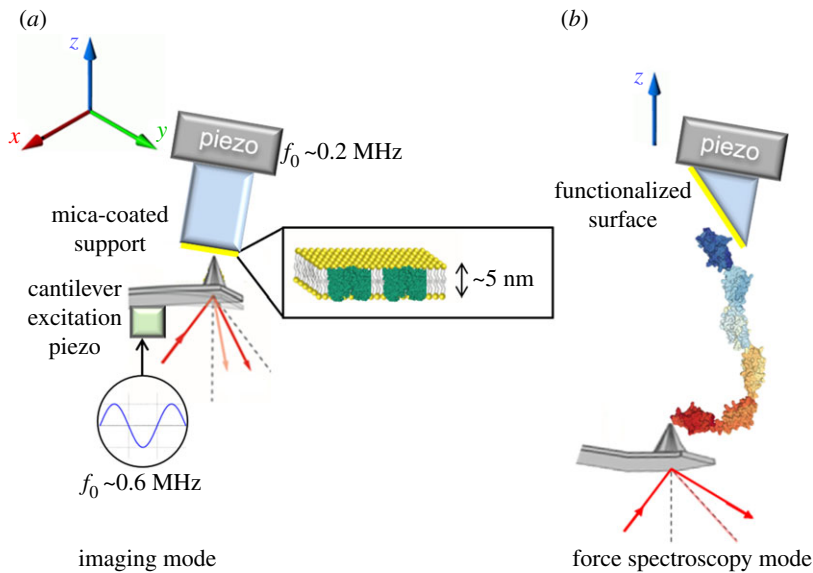


Figure 1. Schematics of HS-AFM systems for imaging (a) and force spectroscopy (b). For high-speed AFM imaging, the cantilever is excited through a small piezo element near its resonance frequency (approx. 0.6 MHz in aqueous solution). For flat surfaces such as biomembranes (schematized in the inset with outer membrane protein PDB code: 3POQ) the sample is scanned in the horizontal plane (xy) and the cantilever deflection is monitored by a photodetector which collects the reflection of a laser beam focused at the back of the AFM cantilever. Topographical images are obtained from the continuous correction of the z movement to keep the amplitude of oscillation constant using a feedback controller. In the case of force spectroscopy mode, the sample approaches to and retracts from the sample in the vertical direction and the force between the tip and the sample is determined from the cantilever deflection. The sample may be tilted to further reduce the effective viscous drag coefficient of the cantilever near the surface. Functionalized surfaces and cantilever tips are often used to probe the mechanics of single molecules, such as multidomain proteins (the I-band fragment I65–I70 from titin, PDB code: 3B43, is shown). (Online version in colour.)

- (4) *Adaptive/dynamic feedback.* during fast imaging, the tip tends to ‘detach’ completely from the surface at the downhill regions, an effect known as *parachuting*. To address this, a dynamic controller was developed, consisting in a feedback controller that increases automatically the gain when downhill regions are scanned.

HS-AFM has been also adapted to perform HS-FS. When AFM is operated in force spectroscopy mode, the tip approaches and retracts perpendicularly from the surface at controlled force and velocity. This allows detecting specific interactions using functionalized tips and probing mechanical properties of single molecules, membranes and living cells. The miniaturization of the cantilever in HS-AFM results in a very low viscous damping, which is a prerequisite for a μ s-response time. In fact, the components and their miniaturization necessary to perform HS-FS are equivalent to those of imaging. Another technical particularity to improve the performance of HS-FS is to tilt the surface 45° , minimizing the effective viscous drag of the cantilever. With this configuration, it is possible to reach pulling velocities up to approximately 30 mm s^{-1} [43,44]. Such recordings required analog-to-digital converter with high temporal resolution (tens of megasamples/s). Other technical modifications have been explored allowing the use of new methodologies with the HS-AFM set-up for improved mechanical measurements. Smaller z -piezo actuators give access to high frequencies (up to 120 kHz) in order to probe the microrheology of soft samples at high rates [45]. The use of torsional harmonic cantilevers allows also force measurements of receptor/ligand bonds with μ s-time resolution [46]. Micromachining of ultrashort cantilevers also remarkably improves force sensitivity while maintaining μ s response time [47].

213 Particularly in the case of operation on cells, AFM systems are usually coupled to optical
214 microscopes. This helps to position the AFM cantilever over the cell and to visualize major
215 changes. In order to visualize the cells while maintaining the performance of HS-AFM, a prism
216 was used on top of the z-piezo, where the sample stage is mounted. This allowed transmitted
217 illumination of the sample [45,48]. In that case, a 'sample-scanning' set-up was used, in which the
218 sample moves with the piezoelectric components while the cantilever is fixed -this configuration
219 is mechanically stable. Nowadays, there are already commercial 'tip-scanning' HS-AFM set-ups,
220 in this case, the tip moves relative to the sample and therefore an inverted optical microscope can
221 be easily coupled, allowing advanced approaches such as total internal reflection fluorescence
222 microscopy [49].

223 Still, HS-AFM remains a surface technique, so the molecules of interest need to be adsorbed
224 or immobilized on a substrate. This, in turn, may restrict the dynamics and natural interaction
225 between biomolecules. Even so, molecules diffusing faster than the frame rate cannot be imaged
226 by means of HS-AFM. Thus, for each system to be studied by HS-AFM, the conditions of sample,
227 medium and substrate need to be optimized.

228 Combination of FS and imaging modes leads to approaches such as force mapping in
229 which force curves are acquired at different locations across the sample surface to obtain
230 multiparametric maps revealing, for example, elasticity or adhesion [50]. While the application
231 of HS-AFM for force spectroscopy-based mapping is still not mature, some recent works point
232 towards this direction [33,51–53].

234 3. Biological physics explored by HS-AFM

236 (a) Dynamic organization of membranes

237 The cell membrane is the fundamental support matrix and ultimate energetic barrier of the cell.
238 In biological membranes lipids mainly organize in lamellar phases, where acyl chains of two
239 different lipid leaflets align oppositely to form a hydrophobic core and the polar headgroups
240 remain exposed to the water interface. Since the discovery of lamellar phases in cell membranes
241 [54], many attempts have been done -and still do- to explain the lateral heterogeneity of
242 membranes through relevant physical-chemical features. The two most outstanding hypothesis
243 in the field are the fluid-mosaic model by Singer and Nicolson in 1973, depicting cell
244 membranes as two-dimensional liquids where all lipid and protein molecules diffuse easily
245 [55], and the lipid-rafts hypothesis proposed in 1997 by K. Simons and E. Ikonen [56], which
246 depicted functional lipid patches -rafts- in the two-dimensional fluid matrix. Nowadays, it is
247 well known that there are a variety of nanostructures in the membrane of heterogeneous sizes and
248 functions, and the methods that allow us to observe these nanodomains *in vivo* are only starting to
249 emerge [57]. HS-AFM represents now a major tool to study the dynamic organization of biological
250 membranes.

253 (i) Phase transition of lipid membranes

254 Comparable to cell membranes, biomimetic membranes, typically studied as supported lipid
255 bilayers (SLBs) or vesicles in suspension, adopt different phases: solid (gel phase) and fluid
256 (liquid-ordered and liquid-disordered phases). The occurrence of these phases depends on
257 the lipid nature, temperature and environmental conditions. First-order transitions of lipid
258 membranes are well known, at low temperatures lipids are arranged on a triangular lattice,
259 known as solid phase (or gel phase or L_{β}). By contrast, at high-temperature lipids are in the liquid
260 phase (or fluid phase or L_{α}), reflecting the order-disorder transition of the hydrocarbon chains
261 of the lipids. Some lipids present a pretransition before the main first-order transition which give
262 rise to an intermediate order in the lipid bilayers referred to as ripple phase (P_{β}'). Ripple phases
263 are smectic phases characterized by structural periodic corrugations. AFM imaging revealed the
264 structure of ripple phases in hydrated conditions at the nanometre scale [58]. The observation of
265

a phase transition process is characterized by a melting point temperature of the ripple phase to fluid phase, nucleation point and growth directionality for the formation of the ripple phase.

HS-AFM coupled to a temperature-controlled system reported directly ripple to fluid phase transitions (reversibly) in real time and at high resolution [59]. When the fluid bilayer was cooling down, ripples appeared as concentric rings progressing from the edge region of the lipid patch towards the centre upon cooling. This ring-pattern formation was maybe a consequence of a heterogeneous thermalization along the nanometric patch and cooling progressed from the edges that expose the largest surface to the cooling bulk. It could also be a consequence that the bending and edge formation of the lipids at the patch border represented favourable nucleation spots for ripple phase reformation. In fact, throughout cycles of heating/cooling, the ripple phase pattern changed every time suggesting that the thermal history of the bilayer was erased in the fluid phase. Based on the van't Hoff expression, the representation of area fraction of each phase as a function of the temperature provides estimations about the transition enthalpy and the cooperativity of the lipid molecules during the process. The cooperativity of each process also accounts for the order of the transition, more cooperative processes relate to first-order transitions, where the latent heat is required to change the phase, while in second-order transitions heat is also necessary for changing the temperature. Ripple phase melting occurs at locations where ripple pattern interfaces (disorders) are detected. These disordered areas probably comprised a slightly higher amount of liquid-like lipid molecules and hence present ideal locations for initiation of melting or nucleation of the meta-stable ripple phase. Furthermore, the local transition of the bilayer into fluid phase, i.e. a complete mixing of the lipids at high lateral dynamics, leads to a 'loss of memory' of the bilayer. The correlation of nanoscale thermotropic transitions with micro and mesoscopic thermodynamic descriptors, as the enthalpy of the process, helps to further understand the system. A lipid membrane containing small domains does not necessarily correspond to a phase coexistence regime, but it may constitute a one phase regime with micro- or nanoscale heterogeneities. In this sense, HS-AFM observations may help filling the gap between single-molecule diffusion studies to the collective migration of lipid domains or patches. This could have implications for more complex cellular systems where lipid nanodomains form and dissociate reversibly.

(ii) Fractality

The cell membrane is an intrinsically complex and dynamic bidimensional fluid densely crowded with proteins on which ordered patterns do not dominate. Individual membrane proteins participate at more than one function. Therefore, by combinatorial, the number of functions of the membrane proteins is higher than the number of membrane proteins. Fractal geometry is a useful mathematical tool to understand the interaction of multiparticle systems and characterize systems with several characteristic lengths or levels of construction. Fractal geometry is defined by the fractal dimension (D). For membrane proteins, the more fragmented the spatial distribution of the proteins, the higher D . Fractal geometry has, for example, been used in biology to describe plants or cardiovascular vessels. It has been shown that higher values of fractality reduce the energy requirement for the distribution of resources [60–62]. At the molecular scales, the role of fractality is less well understood. On the cell membrane, the assessment of fractality has been 'blind' and indirect, calculated from models and observations of diffusing biomolecules tagged with fluorescence markers [63,64]. The basic idea is that the geometrical partitioning of the membrane (dangling ends, bottlenecks and backends) generates restricted areas of diffusion and interaction and inter-connectivities between the membrane proteins that have dramatic effects on the biochemical kinetics of the cell membrane. Mathematically, on fractal arrangements, the number of sites that a random walker molecule visits in N motion steps is proportional to the fractal dimension (so, the number of visited sites $\sim N^D$) [65]. Therefore, in the areas of the membrane of partitioning of higher fractality, the protein diffusion searches 'more carefully' the space and minimizes the chances of missing a target in the close vicinity.

The HS-AFM concomitant visualization of diffusion and the surroundings is an ideal tool to study the fractality of the plasma membrane and the correlation of protein–protein interactions with the organization of the membrane [66]. HS-AFM videos of the spatio-temporal distribution of the bacterial channel outer membrane porin F (OmpF) on membranes [67] showed that the trimers of OmpF arrange in an intricate geometry with a high fractal dimension $D \approx 1.73 \pm 0.01$, a value of D characteristic of particles performing a random walk and sticking together the moment they touch. This process of fractal formation known as diffusion limited aggregation (DLA) [68,69] provides a wide variety of local environments that promote, for example, translocon complexes [70] or that ensures that the fluxes of matter that cross the OmpF are evenly distributed across the bacterial plasma membrane and arrive consuming minimal energy to all the cell. For comparison, a simulation of the OmpF trimers arranged in a two-dimensional array had a fractal dimension of $D \approx 1.05 + 0.02$, so the OmpF arrangements expose about twice as much molecular surface as molecules in a regular array. Besides DLA, another physical process that can produce fractal-like membrane partitioning is percolation. When the membrane domains fuse to a single continuous one (percolation threshold), fractality appears at short distances, but the distribution is homogeneous at larger length scales, two different temporal diffuse regimes appear at this moment across the membrane [71]. HS-AFM may allow the observation of this other fractality processes by allowing dynamic visualization of all the components of a biological system at the nanoscale.

(iii) Glassy mosaic model

As describe above, fractality is a possible approach to quantify the complexity of a system. Two disciplines have evolved side by side in our comprehension natural complexity: biology and condensed matter physics, yet, on the topic of glasses they are distant apart. In physics, the glass transition and glass rheology has been for years one of the ultimate and most blurry and undefined frontiers and the literature at this respect is vast [72]. On the contrary, biology mentions to glasses are sporadic at best. Probably, scale is the most relevant factor that explains such discrepancy. Glass rheology experiments track particles in the micrometre to millimetre scale, where particles are easy to visualize. By contrast, protein tracking experiments using fluorescence microscopy take place at the nanoscale where tracking is challenging. In addition, the spot size of the fluorescence tag used to track biomolecules, approximately 200 nm, is too large to distinguish the collective motions of neighbouring molecules. Because glasses originate in collective dynamics that emerge when particles cluster in a short time creating a long-lasting non-equilibrium, glass dynamics is difficult to identify using fluorescence particle tracking [64]. Another factor that may have kept glasses out of the radar of biology is that the trajectory of a particle in a glass looks (at experimentally available times) just like the trajectory of the biomolecules interacting with their surroundings, leading to what is known as anomalous diffusion.

HS-AFM offers a unique possibility to assess glassy states in biological membranes as it enables video imaging of the totality of molecules in the ensemble. Using HS-AFM [73], it was shown that glassy states appear in biological membranes on assemblies of lysenin, a pore forming toxin from the coelomic fluid of the earthworm *Eisenia fetida*. Lysenin binds and readily forms clusters in the lipidic membrane domains of the targeted cells [73–75]. HS-AFM data showed that the glassy state interconnects membrane regions of solid and fluid character. In the glassy regions, cages of neighbours obstruct the diffusion with a characteristic time, a few seconds, which regulates the flow of particles across the glassy zones. Diffusion was non-Gaussian at lag-times smaller than the characteristic time and Gaussian at longer lag-times. Such glassy areas were observed by HS-AFM to surround the solid 2D crystal and, thus, to define the exchange rate with the free Gaussian diffusion regions (figure 2).

We can ask ourselves which evolutionary advantage an organism could obtain from the use of glassy states. We can think that the organisms could create glassy states to stop and reactivate their molecular ensembles without any requirement for large structural transitions, as it is the case if phase transitions are used as a molecular clock that tic at the pace of

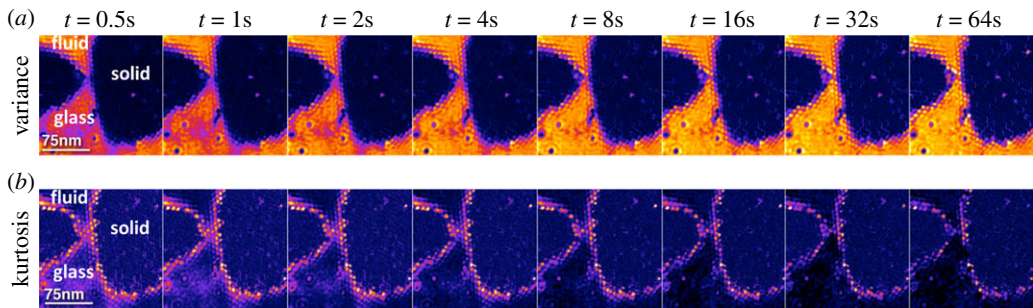


Figure 2. Glassy states in biological membranes. Areas of non-Brownian dynamics of lysenin toxin on supported lipid bilayers identified by HS-AFM topographic movies. The different time-lags show variation of the (a) variance (V) of the distribution of height changes (false colour scale: $0 < V < 2$ nm) and (b) kurtosis (K) (non-Gaussianity) of the distribution of the height changes (false colour scale: $2.5 < K < 5.0$). Adapted from [73]. (Online version in colour.)

ageing of collective phenomena. As a matter of fact, some molecular trajectories detected in living cells, described using the formalism of continuous-time random walk [76], which considers a continuous distribution of waiting times between trajectory steps, could be due to the diffusion of the molecules in a glassy state [77]. Future experiments may allow us to observe other properties of glassy systems, such as ageing, and lead to the description of the membrane as a *glassy mosaic model*.

(iv) Protein self-assembly during fission membrane remodelling

The potential of HS-AFM technology transformed our understanding of protein self-assembling in membranes. During membrane remodelling, there are -generally speaking- two sort of events, fusion and fission, which give rise to topological changes. The topological invariant is described by the Euler number, which is decreased during fusion, when two vesicles merged, or increased during fission, when two vesicles divide. Membrane remodelling events are then classified based on the topological changes and the location during the remodelling process [78]. Thus, external changes are led by proteins located on the external leaflet of the membrane budding neck, and internal are those driven by proteins which assemble in its lumen.

Concerning internal fission in membrane remodelling, a successful HS-AFM study was focused on the endosomal sorting complex required for transport-III (ESCRT-III) [79]. This complex-based machinery is highly evolutionary conserved, and it is required for lipid membrane remodelling in many cellular processes, from abscission to viral budding and multi-vesicular body biogenesis. Snf7, the major component of ESCRT-III, polymerizes as a spiral transiently in the membrane (figure 3), inducing curvature which eventually will contribute to bud and constrict the membrane. The model proposed in [79] for deformation and budding induction relies on the elastic relaxation of the ESCRT-III polymer. HS-AFM observations showed that Snf7 flexible filaments have a preferred curvature radius, hence growing as a flat spiral onto the lipid membrane they accumulate elastic stress. The external filaments of the spirals-disks are underbent, the more it polymerizes, the higher the energy it accumulates. By measuring the polymerization energy and the rigidity of Snf7 filaments, HS-AFM videos showed that the elastic expansion of compressed Snf7 spirals could stretch the lipids they are bound to, generating an area difference between the membrane leaflets (buckling) and, thus, inducing curvature. This spring-like activity of ESCRT-III is, to our knowledge, new to the field of membrane remodelling. HS-AFM also provided high-resolution films of the enzymatic disassembly of ESCRT-III by the ATPase Vps4 [80]. In the presence of a pool of soluble Snf7, ESCRT-III assemblies shrank under the action of Vps4, liberating free space on the membrane where new ESCRT-III assemblies were growing simultaneously. This results in turnover and high lateral mobility

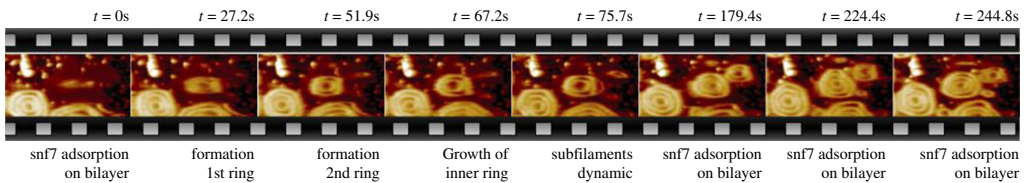


Figure 3. HS-AFM movie frames showing how Sn7, the major polymerizing component of ESCRT-III, assembles as a flat spiral disk on flat lipid membranes. Sn7 spirals can function as spiral springs. Using HS-AFM, the polymerization energy and the rigidity of Sn7 filaments were estimated, showing that they were deformed while growing in a confined area. The elastic expansion of compressed Sn7 spirals could stretch the lipids they are bound to, generating an area difference between the membrane leaflets and thus curvature. This spring-like activity underlies the driving force by which ESCRT-III could mediate membrane remodelling. For insights, see [79]. (Online version in colour.)

of ESCRT-III assemblies on membranes. Dynamic turnover provides an explanation for how ESCRT-III filaments gradually adapt their shape during membrane constriction, which has broad implications in diverse cellular processes, differing in size, shape and duration—such as plasma membrane repair, cytokinesis or viral budding.

External fission has been extensively described for the dynamin machinery, which assembles as a helix in the external part of the budding neck. Dynamin is a GTPase motor and its constriction is essential for cell events such as endocytosis and organelle division. However, the mechanism of constriction and twist by the dynamin helix has been thoroughly debated. The complexity arises from the fact that the dynamin polymer has both contractile and torsional abilities, involving changes of contiguous dimers at the molecular level but also at the whole polymer level—changes not accessible by standard structural biology tools. HS-AFM allowed the visualization of the constriction of single dynamin-coated membrane tubules [81,82], showing the distance between the helix turns and between dimers along the polymer. These distances were shown to vary over time, as helical turns were observed to transiently pair and dissociate. This hampers the propagation of constriction along the length of long helices. Eventually, local fission occurs only where constriction is the strongest. At fission sites, these cycles of association and dissociation were correlated with relative displacement of the turns and constriction. HS-AFM findings support a model in which conformational changes at the dimer level drive relative sliding of helical turns, and constriction by torsion.

The application of HS-AFM on biological membranes ~~allowed~~ contributed to our understanding of biological function through physical descriptions of the molecular processes and, importantly, allowed the observation of emergent physical phenomena.

(b) Molecular machines

The last examples reveal the importance of chemical energy-driven processes in biological function. The proteins that run most of these processes are often known as molecular motors. Molecular motors are the scientific leitmotif that drove Toshio Ando at the University of Kanazawa to invest a decade of efforts in the development of HS-AFM. Molecular motors are biomolecules capable of generating directed motion by taking energy from the statistical fluctuations that surrounds them, thanks to an asymmetric energy landscape with respect the spatial direction of displacement. In addition, the activity cycle of molecular motors include one or several irreversible gating steps (that convert energy of low entropy into higher entropy energy), forcing the motor to move forwards. Even if the ruling principles of the physics of molecular motors are known, each motor has evolved to develop its own strategies of implementation, which adapt better to a specific function. Many details of their functioning are controversial and different experiments have resulted in different conclusions. Many of these

478 discrepancies originate from the lack of simultaneous measurement of the conformational and
479 chemical changes of molecular motors.

480 One of the motors whose mechanism of functioning is still unclear is myosin V. Myosin V
481 puzzles because the experimental data suggests that the gating step in its mechanism takes place
482 in the opposite sense to what would be expected from its directional motion: it takes place
483 simultaneous to the attachment of the motor to the filament, a favourable event that does not
484 require additional free energy contributions. Why myosin V supplies even more energy at this
485 step is unclear. Other molecular transport motors, like kinesin use the free energy supplement
486 of ATP hydrolysis to detach the motor from the molecular track. The predominant hypothesis is
487 that myosin V stores the energy supplied by the ATP hydrolysis in the form of mechanical energy
488 creating intermolecular stress. The activity of myosin V was filmed at the molecular scale using
489 the HS-AFM by Ando *et al.* [83]. This was the first-ever detailed assessment of the time-lapsed
490 sequence of structural configurations of myosin V, out of reach to other techniques previously
491 used to characterize molecular motors (fluorescence microscopy, laser tweezers, X-rays or electron
492 microscopy). The HS-AFM data provided new insight on the debated myosin V mechanism of
493 action: it showed that the creation of intermolecular stress in the myosin V structure can be
494 induced by the simple attachment to the actin filament, and that not extra free-energy from the
495 ATP was required. HS-AFM data suggests that the free energy supplement could be exclusively
496 required to break the bond formed to the actin filament, as in the case of the kinesin motor. At the
497 present time, the precise mechanism of myosin V remains unclear.

498 ATP synthases are rotary catalytic molecular machines ubiquitous in organisms from plants to
499 amoeba to humans that produce ATP from ADP. During its rotation the ATP synthase modifies
500 the shape of its enzymatic pockets, and there are three structural-enzymatic steps related to
501 the different rotation angles (the binding of an ADP and a phosphate, the attachment of the
502 phosphate, and the release of ATP). The free energy required for the synthesis of ATP from ADP
503 is provided by the flow of protons that moves across the molecule (the proton-motive force).
504 Taking advantage of the HS-AFM fast imaging, it was possible to conclude that the F1 domain
505 of the ATP-synthase is capable of performing its structural transitions independently of the F0
506 domain. The HS-AFM movies show isolated F1 domains undergoing the structural transitions of
507 its activity cycle [84]. It had been previously hypothesized that the rotation of F0 controlled the
508 enzymatic activity of F1. HS-AFM showed that F1 can structurally cycle independently of F0. The
509 HS-AFM video imaging also enabled the first-ever AFM imaging of ATP-synthases on bacterial
510 membranes diffusing on close proximity to the proton-pump machinery (the bacteriorhodopsin
511 proteins) and supramolecular organizing in short-lived assemblies of two molecules (dimer)
512 [85]. The oligomerization of the ATP-synthase is believed to help its function as by a mutual
513 compensation of the torque forces the rotors exert on the membrane [86]. Moreover, in this work,
514 the fast frame rate and the nanometre resolution of HS-AFM provided a method to determine
515 membrane-mediated interaction of integral membrane proteins, a method not accessible to other
516 tracking techniques.

517 Another interesting molecular motor is the helicase domain of DNA-modifying enzymes,
518 such as restriction enzymes. During DNA translocation, this motor puts in contact two distal
519 DNA sites. HS-AFM observations revealed two mechanisms of communication of the two DNA
520 sites: passive diffusion of the protein over the DNA -which depends, in turn, on the DNA
521 persistence length- and specific protein binding [87]. The capacity of HS-AFM to visualize
522 dynamic conformational changes in proteins is currently shifting our perspective of structural
523 biology by introducing the dimension of time.

524 (c) Dynamic (un)folding of proteins

525 A functional protein, such as myosin V described above, often requires the folding of the
526 polypeptide chain into the secondary and tertiary structure. Understanding of this folding process
527 is a challenge in biology, but also from a physical point of view. Already in 1968, Cyrus Levinthal
528 proposed a paradox that suggested that the time required for a protein to fold into its native
529
530

state from a random exploration of its configurational space should be exceptionally long [88]. However, it is known that proteins can fold within seconds or less. While different mechanisms have been proposed, the process by which proteins find their native folded state is still largely unknown and represents a tempting challenge for physicists. Indeed, a large number of works have tried to decipher the folding or unfolding process of proteins using different experimental and theoretical tools.

An important conceptual advance in our understanding of protein folding was the introduction of the concept of funnel-shaped, rough energy landscape by Frauenfelder *et al.* [89]. Early experiments by Frauenfelder and co-workers used photolyzing over nine decades in timescale to observe the rebinding of CO to myoglobin [89,90]. The authors were able to observe the relaxation and the conformational changes undergone by the protein upon rebinding of CO in a process that resembled quakes. This led to the concept of a multi-tier, rough energy landscape in which proteins jump from substate to substate thanks to thermal motion. The concept took advantage of advances in the field of spin glasses, revealing again the importance of the dialogue between physics and biology [91]. The funnel shape assures that the protein is directed towards substates of lower and lower energy avoiding frustration [11]. This idea allows to somehow reconcile the mechanism of protein folding in a similar way, with the protein diffusing down the energy landscape in search of the native state. As we will see below, the concept of energy landscape will allow us to interpret protein (un)folding processes probed by HS-AFM.

(i) Intrinsically disordered proteins

While most known proteins present a folded state, intrinsically disordered proteins (IDPs) represent a large family of proteins whose structure is not stable and most of the polypeptide chain is disordered. In addition, structured proteins often contain disordered regions, which appear as blurred electron density maps in X-ray or cryoEM data. IDPs have even been defined as 'protein clouds' invoking their dynamic nature and lack of secondary or tertiary structure, but as an ensemble of structural conformations not directly accessible in conventional high-resolution structural approaches [92]. Study of this particular proteins is still a challenge. HS-AFM is likely the only technique capable of visualizing the dynamic structure of IDPs [93]. An important contribution towards a visualization of unfolded proteins was reported on IDPs [93–95]. In the work by Miyagi and co-workers, the authors studied facilitates chromatin transcription protein (FACT), a protein with predicted large ID regions that facilitates RNA polymerase II transcription and chromatin remodelling [94]. HS-AFM imaging at a remarkable 5–17 frames per second of immobilized FACT revealed a stable lumpy structure, flanked by long tail-like structures that underwent rapid fluctuations (figure 4). Analysis of the contour length of the fluctuating regions and using deletion mutants allowed them to identify the tail structures as the two major ID regions. Moreover, analysis of the root mean squared point-to-point distance of the tail-like structures as a function of the contour length provided a measure of the elasticity of these ID regions by using statistical polymer chain analysis to obtain the persistence length (l_p). Interestingly, the reported $l_p \sim 10$ nm was much larger than the value usually obtained in force-extension curves of unfolded proteins (approx. 0.4 nm), suggesting higher stiffness [96–98]. Making IDPs stiffer (larger l_p) would indeed lower the probability of reaching compact, folded structures by limiting the number of accessible states. This is likely accomplished through electrostatic repulsion between charged residues, abundant in IDPs [99]. IDPs seem to have evolved to avoid a funnel energy landscape and remain within a tier of states with similar energy, still avoiding misfolding and, perhaps, taking advantage of frustration [100].

(ii) Forced protein unfolding at μ s time scales

Another approach to study folding and unfolding of individual proteins is force spectroscopy (FS) [21,96,101]. The adaptation of HS-AFM allows now FS experiments at high velocities with μ s time resolution [102]. Unlike AFM imaging that try not to perturb the proteins, FS of protein unfolding consists in grabbing a protein with the probe, pulling from it at constant velocity and measuring

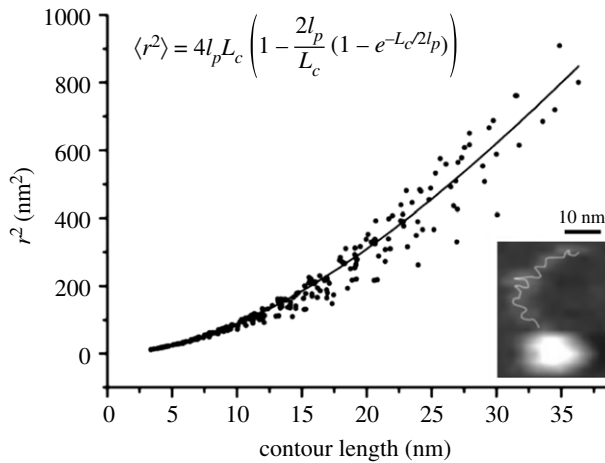


Figure 4. Intrinsically disordered FACT proteins visualized by HS-AFM imaging. The mean squared point-to-point distance (r) of tail-like structures measured from movie frames (insert) as a function of the contour length (L_c) allows determination of the macroscopic persistence length (l_p) using the appropriate chain polymer model (equation). The insert shows a movie frame revealing a FACT protein with the contour length of the tail-like region schematically depicted. Adapted from [94].

the force required to unfold it. Early experiments by the group of Hermann Gaub revealed that certain protein domains, such as the immunoglobulin-like (I) domains of titin formed by β sheets, unfold in an abrupt manner in a reversible processes that was described with just two states: the native, folded state and the unfolded state [21]. Being a thermally activated process, these unfolding forces depend on the pulling rate, actually on the rate of force increase or loading rate (figure 5). The Bell-Evans model allows to model this process and characterize the energy barrier in terms of a distance to the transition state (x_b) and an intrinsic unfolding rate (k^0) from the fit to the spectrum of unfolding force versus loading rates [105]. A large number of experiments have shown that, while the intrinsic unfolding rate ranges several orders of magnitude, the distance to the transition state lays within a narrow range of values between approximately 0.1 nm to approximately 2 nm [96]. The interpretation of this distance from a structural point of view is still a matter of debate and reaching a microscopic understanding will certainly require combination of MD simulations. Indeed, MD simulations of forced unfolding provide an atomic description of the process. However, the computational cost of MD simulations did not allow pulling at the same velocity applied in experiments, not allowing direct comparison of the unfolding forces [106]. In an effort to bridge this gap, HS-AFM was adapted to allow HS-FS [43]. The first HS-FS experiments pulled on the I91 domain of titin at velocities up to approximately 4 mm s^{-1} , more than 100 times faster than conventional AFM, reaching the lower range of velocities probed by all atom MD simulations. The unfolding forces measured over five decades in pulling velocity revealed a logarithmic response with an upturn at the highest velocities and predicted an energy landscape with $x_b \sim 0.89 \text{ nm}$ and $k^0 \sim 2 \times 10^{-10} \text{ s}^{-1}$ (0.45 nm and $7 \times 10^{-6} \text{ s}^{-1}$ if using the loading rate, figure 5). This distance was remarkably larger than earlier results (approx. 0.25 nm) but closer to the extension at which titin lose their tertiary structure (1.1–1.4 nm) reported by MD simulations [103,106]. HS-FS was also applied to unfold spectrin repeats, α -helical domains. In contrast to titin, HS-FS revealed a distance of approximately 0.5 nm, much lower than the distance at which tertiary structure breaks (approx. 5 nm) as revealed from MD simulations [107]. It is important to note that other theoretical models may lead to different values of x_b and k^0 and that several combinations of these two parameters may lead to good fits [108]. Thus, while theoretical models allow us to obtain a phenomenological picture of protein unfolding, only the combination with MD simulations will provide the necessary hints to a microscopic interpretation [109]. As we

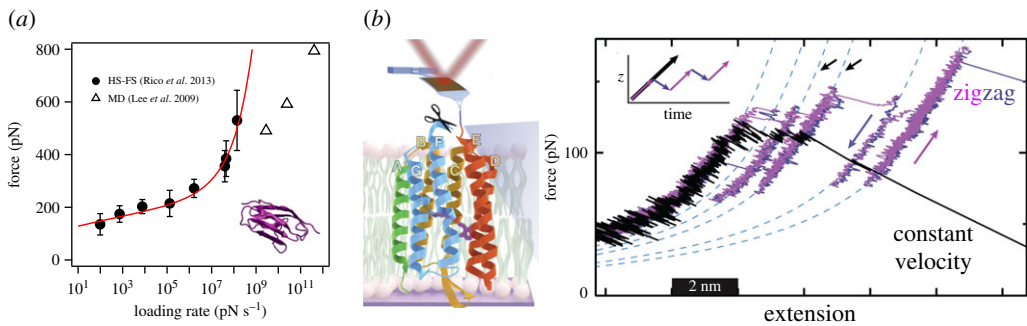


Figure 5. High-speed force spectroscopy. (a) DFS of titin I91 domain unfolding from HS-FS experiments [43] and MD simulations (open triangles, [103]). The inset shows the crystal structure (pdb code: 1TIT). The red solid line is the best fit to the BSK model with parameters $k^0 = 7 \times 10^{-6} \text{ s}^{-1}$, $x_b = 0.45 \text{ nm}$ and $\Delta G^\ddagger = 25 k_B T$. (b) Bacteriorhodopsin unfolding from zigzag experiments using modified ultrashort cantilevers (left). Force-extension curve revealing different intermediate states being visited during both extension (purple) and release (black) trajectories (adapted from [104]). (Online version in colour.)

will address below, only a dialogue between experiments, theory and simulations will reconcile microscopic and phenomenological interpretations.

An advantage of single-molecule techniques is the capacity of observing transient events and exploring intermediate states that may be averaged down in bulk measurements. Intermediates states have been observed using FS, including on titin and spectrin [110,111]. The application of HS-FS represented a step forward in our understanding of these intermediate states. In the first study reporting intermediates of titin I91, the authors combined AFM with MD simulations, which allowed them to interpret a pronounced hump before complete unfolding during extension as the disruption of a β -strand that extended approximately 0.7 nm. Later studies revealed that the force at which this hump appeared was rate-independent and acted as a force buffering mechanism to prevent titin domains from complete unfolding [112]. HS-FS confirmed this rate-independent behaviour up to a certain velocity, upon which the force followed the usual logarithmic dependence [43]. These results were interpreted as two different dynamic regimes: a near-equilibrium regime in which folding and unfolding compete, and a thermally activated regime above a certain velocity, at which refolding became negligible due to the high force reached. A similar mechanism was found for spectrin repeats in which the dynamic equilibrium between unwinding and rewinding of α -helices resulted in a force plateau in unfolding force-distance curves [107]. Observation that was supported by MD simulations which revealed unwinding/winding events at the slowest velocities. These works revealed the dynamic nature of small secondary structures such as β -strands and α -helices, which constantly assemble and disassemble due to thermal motion in dynamic equilibrium, equilibrium broken by mechanical force.

Membrane proteins are particular because they live within the lipid bilayer of the membrane and mechanical unfolding involves also extraction from the lipid environment. In their early work, Oesterhelt and co-workers used AFM to image and mechanically extract and unfold bacteriorhodopsin (bR), an α -helix rich protein that works as a proton pump in purple membranes [113]. The results revealed that the unfolding pathways of bR correlated well with the orientation and organization of the protein, with two pairs of helices (GF and ED) unfolding pairwise and another pair (BC) occasionally unfolding sequentially. Interestingly, the authors already predicted that 'better instruments should allow an even more detailed interpretation of the unfolding pathways'. Indeed, recent work by the Perkins group used ultrashort HS-AFM cantilevers modified using focused ion beam (FIB) to unfold bR [114]. FIB modification of ultrashort cantilevers enhances importantly the force sensitivity while keeping μs response time [47]. This allowed the authors to revealing more complex bR unfolding pathways. While the original

work on bR suggested 3 or 4 intermediate states, Yu and co-workers identified as many as 14 intermediate states only in the unfolding of the ED helix pair. Moreover, the relatively slow pulling velocity applied (300 nm s^{-1}) and the improved temporal and force resolution allowed observation of quasi-equilibrium fluctuations between states separated only by one α -helical turn and with dwell times down to $8 \mu\text{s}$ (potentially $3 \mu\text{s}$). Furthermore, by retracting the cantilever at predefined steps, equilibrium experiments at constant force allowed visualizing the back and forth transitions of a single alpha-helical turn within approximately $15 \mu\text{s}$. These equilibrium trajectories allow them to reconstruct the energy landscape for the unfolding of one α -helix turn, resulting in an unusually high energy barrier of approximately $4.7 k_{\text{B}}T$. Notably, this work resolved long-standing discrepancies between conventional AFM experiments and MD simulations [115], again corroborating that the complementarity of experiments and simulations is optimally achieved if both techniques probe the system at similar time scales. In an intelligent approach, Jacobson and co-workers applied zigzag extension curves to the same bR system to allow repetitive sampling of the various intermediate states, enhancing importantly the statistics and revealing previously hidden states [104] (figure 5). It would be interesting to see if the number and location of the visited states remains constant or it rather varies by changing loading rate as simulations predict [115]. As pointed by the authors [114], HS-FS studies seem to challenge the notion that most SMFS experiments of protein unfolding occur far from equilibrium, while refolding has been observed in titin, spectrin and bR unfolding. Temporal resolution, thus, matters and provides a better understanding of the complex process of protein folding.

(d) Single-molecule mechanics at the shortest timescales: bridging experiments, theory and simulations

As seen in the previous section, experiments, theory and MD simulations have walked together since the beginning of SMFS. The first FS experiments determining the rupture forces of (strept)avidin/biotin (SA/b) bonds were rapidly followed by theoretical developments and MD simulations that allowed us to interpret the reported rupture forces [17,105,116,117]. On the one hand, theoretical models provided a phenomenological understanding based on the concept of energy landscape. As described above for protein unfolding, unbinding was also modelled as a barrier crossing process from the bound to the unbound state, in which the barrier height was lowered by the applied force. This allowed predicting the dependence of the unbinding/unfolding force as a function of loading rate. The Bell-Evans model established a logarithmic dependence of force versus loading rate that allowed the determination of the energy landscape parameters x_b and k_0 [105,118]. Finally, MD simulations provided a description of the atomic details. MD simulations can be seen as a nanoscopic attainment of Laplace demon in which the equations of motion of all the atoms of the system are numerically solved at each time step (usually of ~~approx.~~ ~ 2 fs) [103]. The series of time steps result nowadays in μs -long trajectories with accurate knowledge of the relevant events during unbinding or unfolding processes. Due to the high computational cost, in the case of SA/b, the original MD simulations were carried out at pulling velocities orders of magnitude higher than in experiments, thus, covering very short time scales (ps-ns). This posed an interpretation problem because the simulation forces resulted to be much higher than the experimental ones. The seminal work by Evans and Ritchie already tried 'to bridge the enormous gap in time scales between MD simulations and laboratory experiments' by proposing different dynamic regimes for experiments and simulations. Indeed, different works proposed, in addition to the thermally activated regime of experiments, a drift or deterministic ultrafast regime at the much faster velocities of MD simulations [105,116,119]. In the ultrafast pulling regime, the force would increase, not logarithmically, but as the square root of the loading rate. These works suggested that the forces extracted from experiments and from simulations were not directly comparable, as the theoretical assumptions and approximations depend on the pulling rate. As shown above, HS-FS using ultrashort cantilevers allowed *de facto* bridging the gap between experiments and simulations [43,103]. The reported curved shape of the dynamic force

spectrum (figure 5) suggested that the deterministic regime for titin I91 was reached at a critical force of approximately 350 pN, or a critical loading rate of 10^7 pN s⁻¹. The critical loading rate is defined by the parameters of the energy landscape, as $\dot{F}_c = DF_c/x_b^2$, where $F_c = 2\Delta G^\ddagger/x_b$ is the critical force at which the barrier disappears, D , the diffusion constant and ΔG^\ddagger , the free energy barrier height. This implies that the intrinsic properties of the system define the transition from thermally activated to ultrafast regime. Indeed, HS-FS experiments on spectrin repeats reported a critical loading rate of approximately 10^{10} pN s⁻¹, three orders of magnitude faster than that for titin I91 domains. Soon after this work, a theoretical development by Bullerjahn, Sturm and Kroy, proposed an analytical model (BSK) covering both thermally activated and deterministic regimes [120]. Remarkably, the work considered all possible experimental settings in terms of pulling regimes, spring constants and initial conditions, and improved our understanding of the dynamic force spectra obtained from experiments and simulations. The disappearing of the barrier at a critical force represents, however, a conceptual problem (see electronic supplementary material of ref. [120]). Indeed, when the barrier disappears, it is difficult to define the actual point of barrier crossing, and thus the transition from bound to unbound or folded to unfolded. Moreover, at this point the high-barrier approximation by Kramers is no longer valid. Other theoretical developments allow description of the curvature in the dynamic force spectrum based only on the shape of the energy landscape or the presence of multiple barriers, however, they fail at the critical force [121–126]. The recent Cossio–Hummer–Szabo (CHS) theoretical model is worth noting for its capacity to describe a wide dynamic range covering experiments and simulations using a single barrier [127]. The authors introduced the concept of kinetic ductility to describe the mechanical response of single molecules. Ductility, as opposed to brittleness, allows the energy landscape to gradually stretch upon applied force before barrier crossing. That is, on a perfectly brittle molecule x_b remains constant upon force application, while on a perfectly ductile molecule, x_b will shrink indefinitely with applied force. This allowed the description of the full HS-FS spectrum of I91 unfolding as a thermally activated process in which the Kramers approximation of high barrier holds for a much wider dynamic range, without reaching the deterministic regime. The actual shape and brittleness of the energy landscape is nonetheless only accessible using additional data, like bulk determined k^0 , or provided a wide range of loading rates is available, only possible combining HS-FS and MD simulations. Furthermore, the kinetic ductility model requires a remarkably high diffusion coefficient (or preexponential factor). As shown in the force versus loading rate spectrum (figure 5), the last value at the highest experimental velocity deviates from the expected trend. This deviation was interpreted in the same work by Cossio and co-workers, suggesting that at the highest pulling rates of HS-FS, the limited response time of the cantilever may overestimate the measured forces [127]. Future experiments will verify this prediction. It is, however, curious that the use of cantilevers with the shortest response time raised the question of its very influence in FS experiments. This suggests that pushing the technological limits makes science advance at a faster pace [128].

Both works on titin and spectrin using HS-FS allowed reconsidering other theoretical models. In the case of titin, HS-FS revealed that the forces of β -sheet unfolding (hump) were constant for a range of pulling velocities, for then increasing logarithmically at higher rates. In the case of spectrin, a similar behaviour was observed for the continuous uncoiling process of the α -helices. Given the small dimensions of these two structures, this dynamic behaviour was interpreted in terms of an unfolding/refolding quasi-equilibrium regime at which off and on rates compete. The theoretical model by Friddle, Noy and de Yoreo described this process but considering a virtual state due to the convolution of outer barrier of the energy landscape with the inner barrier of partial unfolding [129]. Again, MD simulations were in agreement with the experimental results. This reinforces the idea that the combination of HS-FS and MD simulations allows a back and forth dialog between the two techniques framed by theoretical models.

HS-FS has been also used to measure the binding strength of receptor/ligand interactions. In the recent work on streptavidin/biotin (SA/b) unbinding, the rupture forces were determined using HS-FS and MD simulations over 11 decades of loading rate [44]. HS-FS probed the forces required to break the streptavidin/biotin bond at velocities up to 30 mm s⁻¹, reaching a loading

rate of approximately 10^9 pN s⁻¹, which overlapped with the slowest velocity simulations. The tetrameric form of streptavidin bound to biotin was used and biotin was pulled through a worm-like chain potential linking the biotin to a virtual spring with the same stiffness as experiments. Thus, simulations mimicked the exact experimental conditions. Again, at overlapping rates, rupture forces showed excellent agreement. Interestingly, the very same simulations on the monomeric form of streptavidin showed poorer agreement, reflecting the advantage of combining experiments and simulations at the very same time scales. The full dynamic force spectrum was not entirely described by a single barrier model but required multiple barriers [44]. Brownian dynamics simulations of a double barrier predicted a critical loading rate of approximately 10^{11} pN s⁻¹, only accessible to MD simulations. This extremely fast critical value is reasonable given the small biotin molecule rapidly diffusing across a short distance before unbinding. While the proposed energy landscape was able to describe the unbinding force spectrum of SA/b over 11 decades of loading rate, it predicted an off rate at zero force (\sim s⁻¹) incompatible with the off rate obtained on bulk experiments (\sim days⁻¹). This advocated for another mechanism that would obstruct and slow down the exit of biotin from the SA pocket, after the second barrier was crossed. Indeed, both HS-FS experiments and MD simulations suggested outer barriers due to side-chain interactions and transient induced fits of SA, all depending on the loading rate. Thus, streptavidin may have evolved to slow down the fast diffusion of biotin outside the binding pocket, favouring rebinding and bringing to the complex its unusually long lifetime. Importantly, the outcomes suggested revisiting old and well-established concepts like the lock-and-key model describing receptor/ligand bonds in terms of rate-dependent induced fits of the protein dynamically wrapping around the moving ligand.

The physical description of the mechanics of cells is inevitably linked to polymer physics, given the polymeric network of the cell cytoskeleton. While single-molecule mechanics is difficult to probe on cells, HS-FS has been also applied to living cells in a series of experiments probing the microrheology of the cytoskeleton at high frequencies [45]. In this work, Rigato and co-workers recovered the well-known viscoelastic response of living cells described by soft glassy rheology at low frequencies (less than 0.1–1 kHz) and extended the viscoelastic range up to 100 kHz. In this high-frequency regime, the response was expected to be dominated by the dynamics of the individual cytoskeletal filaments. Indeed, the reported power-law exponents were consistent with predictions from semiflexible filament theories. In this case, the atomic description of the system using MD simulations is still far given the large size of the system, but coarse-grained models may allow us to better understand this dynamic behaviour [130]. We hope that HS-FS will provide a framework to better understand the inherently dynamic nature of single-molecule mechanics by bringing together experiments, theory and simulations.

4. Conclusion and future perspectives

We have reviewed some examples in which physical phenomena emerge from biological systems and whose description and characterization was less clear before the emergence of HS-AFM. HS-AFM has filmed biomolecules at subsecond framerates, perhaps sufficient for capturing the details of a number of processes, like diffusive crowdedness or macromolecular cooperativity, but too slow for capturing many other biomolecular processes. Such is the case, that even the iconic HS-AFM movie of the walking myosin V required to slow down the motion of the legs ~~to be recorded~~ by introducing obstacles [83]. Thus, faster HS-AFM approaches, likely revising the probe technology, will be required to capture the dynamics of other biomolecular processes, such as the gating of ion channels and the diffusion of small proteins [131]. As reviewed here and elsewhere, the energy landscape of proteins and receptor/ligand bonds is rough, with a hierarchy of substates that are transiently and dynamically visited, substates that can now be directly explored on single molecules using HS-FS at μ s-temporal resolution. Future experiments would allow us to determine if this dynamic equilibrium is coloured by dynamic disorder and heterogeneity [132,133]. It may also allow the detection of fast, transient folded states in IDPs or monitor the complete process of protein folding, where short-lived frustration events may occur,

and glassy dynamics may dominate [134]. Moreover, future combination of other nanotools with HS-AFM imaging may allow observing forced unfolding in real time [26]. The certainly upcoming development of high-speed force mapping will allow us to address dynamic modulation of the mechanics in biological systems, such as proteins, membranes and cells [51]. Proteins and membranes seem to share similarities at different length and time scales and physical concepts such as rough energy landscape and frustration provide a phenomenological understanding of these systems. As computational power increases, MD simulations at experimental, μs time scales will become the norm. Combination of conceptual frameworks with experiments and MD simulations will allow us to reach microscopic description of biological physics phenomena. The dialogue between physics and biology is expected to last and HS-AFM will provide a new tool to moderate it.

Data accessibility. This article does not contain any additional data.


Authors' contributions. All authors drafted and wrote the manuscript.

Competing interests. We declare we have no competing interests.


Funding. This project has received funding from the Agence National de la Recherche (ANR), as part of the 'Investments d'Avenir' Programme (I-SITE ULNE / ANR-16-IDEX-0004 ULNE) to L.R.-M and the European Research Council (ERC, grant agreement no. 772257) to F.R.


Acknowledgements. Please acknowledge anyone who contributed to the study but did not meet the authorship criteria.



References

- Helmholtz H von, Javal É, Klein N-T. 1867 *Optique physiologique, par H. Helmholtz, ... traduite par Émile javal et N.-Th. Klein ...* Paris: V. Masson et fils.
- Galvani L. 1791 D viribus electricitatis in motu musculari: Commentarius. *Bologna: Tip. Istituto delle Scienze*, 1791; 58 p.: 4 tavv. ft; in 4.; DCC. f. 70.
- Schrodinger R, Schrödinger E. 1992 *What is life?: With mind and matter and autobiographical sketches*. Cambridge, UK: Cambridge University Press.
- Block SM, Goldstein LSB, Schnapp BJ. 1990 Bead movement by single kinesin molecules studied with optical tweezers. *Nature* **348**, 348–352. (doi:10.1038/348348a0)
- Collin D, Ritort F, Jarzynski C, Smith SB, Tinoco I, Bustamante C. 2005 Verification of the Crooks fluctuation theorem and recovery of RNA folding free energies. *Nature* **437**, 231–234. (doi:10.1038/nature04061)
- Watson JD, Crick FH. 1953 Molecular structure of nucleic acids. *Nature* **171**, 737–738. (doi:10.1038/171737a0)
- Noji H, Yasuda R, Yoshida M, Kinosita K. 1997 Direct observation of the rotation of F-1-ATPase. *Nature* **386**, 299–302. (doi:10.1038/386299a0)
- Prigogine I, Stengers I. 1979 *La nouvelle alliance: métamorphose de la science*.  Gallimard.
- Mckenzie RH. 2009 Condensed concepts: Biological physics vs. *Biophysics*. *Condensed concepts*.
- Hege H,  Gupta ML. 1973 What is 'Biological Physics'? A resource letter. *J. Biol. Phys.* **1**, 69–122. (doi:10.1007/BF02308973)
- Frauenfelder H, Wolynes PG, Austin RH. 1999 Biological physics. *Rev. Mod. Phys.* **71**, S419–S430. (doi:10.1103/RevModPhys.71.S419)
- Schuler B, Hofmann H. 2013 Single-molecule spectroscopy of protein folding dynamics—expanding scope and timescales. *Curr. Opin Struct. Biol.* **23**, 36–47. (doi:10.1016/j.sbi.2012.10.008)
- Bai X, McMullan G, Scheres SHW. 2015 How cryo-EM is revolutionizing structural biology. *Trends Biochem. Sci.* **40**, 49–57. (doi:10.1016/j.tibs.2014.10.005)
- Svoboda K, Schmidt CF, Schnapp BJ, Block SM. 1993 Direct observation of kinesin stepping by optical trapping interferometry. *Nature* **365**, 721–727. (doi:10.1038/365721a0)
- Neuman KC, Nagy A. 2008 Single-molecule force spectroscopy: optical tweezers, magnetic tweezers and atomic force microscopy. *Nat. Meth.* **5**, 491–505. (doi:10.1038/nmeth.1218)
- Moy VT, Florin EL, Gaub HE. 1994 Intermolecular forces and energies between ligands and receptors. *Science* **266**, 257–259. (doi:10.1126/science.7939660)

Q1

- 902 17. Florin EL, Moy VT, Gaub HE. 1994 Adhesion forces between individual ligand-receptor
903 pairs. *Science* **264**, 415–417. (doi:10.1126/science.8153628)
- 904 18. Smith SB, Finzi L, Bustamante C. 1992 Direct mechanical measurements of the
905 elasticity of single DNA molecules by using magnetic beads. *Science* **258**, 1122–1126.
906 (doi:10.1126/science.1439819)
- 907 19. Bustamante C, Marko JF, Siggia ED, Smith S. 1994 Entropic elasticity of lambda-phage DNA.
908 *Science* **265**, 1599–1600. (doi:10.1126/science.8079175)
- 909 20. Strick TR, Allemand JF, Bensimon D, Bensimon A, Croquette V. 1996 The elasticity of a single
910 supercoiled DNA molecule. *Science* **271**, 1835–1837. (doi:10.1126/science.271.5257.1835)
- 911 21. Rief M, Gautel M, Oesterhelt F, Fernandez JM, Gaub HE. 1997 Reversible unfolding
912 of individual titin immunoglobulin domains by AFM. *Science* **276**, 1109–1112.
913 (doi:10.1126/science.276.5315.1109)
- 914 22. Dunlap DD, Bustamante C. 1989 Images of single-stranded nucleic acids by scanning
915 tunnelling microscopy. *Nature* **342**, 204–206. (doi:10.1038/342204a0)
- 916 23. Liphardt J, Dumont S, Smith SB, Tinoco I, Bustamante C. 2002 Equilibrium information from
917 nonequilibrium measurements in an experimental test of Jarzynski's equality. *Science* **296**,
918 1832–1835. (doi:10.1126/science.1071152)
- 919  24. Binnig G, Quate CF, Gerber C. 1986 Atomic force microscope. *Phys. Rev. Lett.* **56**,
920 (doi:10.1103/PhysRevLett.56.930)
- 921 25. Krieg M *et al.* 2019 Atomic force microscopy-based mechanobiology. *Nat. Rev. Phys.* **1**, 41.
922 (doi:10.1038/s42254-018-0001-7)
- 923 **Q3** 26. Ando T. 2017 High-speed atomic force microscopy and its future prospects. *Biophys. Rev.* **10**,
924 285–292. (doi:10.1007/s12551-017-0356-5)
- 925 27. Ando T. 2017 Directly watching biomolecules in action by high-speed atomic force
926 microscopy. *Biophys. Rev.* **9**, 421–429. (doi:10.1007/s12551-017-0281-7)
- 927 **Q4** 28. Shibata M, Yamashita H, Uchihashi T, Kandori H, Ando T. In press High-speed atomic force
928 microscopy shows dynamic molecular processes in photoactivated bacteriorhodopsin. *Nat.*
929 *Nano* **5**, 208–212. (doi:10.1038/nnano.2010.7)
- 930 29. Preiner J, Horner A, Karner A, Ollinger N, Siligan C, Pohl P, Hinterdorfer P. 2015 High-
931 speed AFM Images of thermal motion provide stiffness map of interfacial membrane protein
932 moieties. *Nano Lett.* **15**, 759–763. (doi:10.1021/nl504478f)
- 933 30. Miyagi A, Chipot C, Rangl M, Scheuring S. 2016 High-speed atomic force microscopy shows
934 that annexin V stabilizes membranes on the second timescale. *Nanotechnol.* **11**, 783.
935 (doi:10.1038/nnano.2016.89)
- 936 31. Marchesi A, Gao X, Adaixo R, Rheinberger J, Stahlberg H, Nimigean C, Scheuring S. 2018
937 An iris diaphragm mechanism to gate a cyclic nucleotide-gated ion channel. *Nat. Commun.*
938 **9**, 1–11. (doi:10.1038/s41467-018-06414-8)
- 939 32. Gilmore JL, Suzuki Y, Tamulaitis G, Siksnyš V, Takeyasu K, Lyubchenko YL. 2009 Single-
940 molecule dynamics of the DNA– Eco RII protein complexes revealed with high-speed
941 atomic force microscopy. *Biochemistry* **48**, 10492–10498. (doi:10.1021/bi9010368)
- 942 33. Nievergelt AP, Banterle N, Andany SH, Gönczy P, Fantner GE. 2018 High-speed
943 photothermal off-resonance atomic force microscopy reveals assembly routes of centriolar
944 scaffold protein SAS-6. *Nat. Nanotechnol.* **13**, 696–701. (doi:10.1038/s41565-018-0149-4)
- 945 34. Preiner J *et al.* 2014 IgGs are made for walking on bacterial and viral surfaces. *Nat. Commun.*
946 **5**, 4394. (doi:10.1038/ncomms5394)
- 947 35. Barrett RC. 1991 High-speed, large-scale imaging with the atomic force microscope.
948 *J. Vacuum Sci. Technol. B Microelectron. Nanometer Struct.* **9**, 302. (doi:10.1116/1.585610)
- 949 36. Viani MB *et al.* 1999 Fast imaging and fast force spectroscopy of single biopolymers with a
950 new atomic force microscope designed for small cantilevers. *Rev. Sci. Instrum.* **70**, 4300–4303.
951 (doi:10.1063/1.1150069)
- 952 37. Ando T, Kodera N, Takai E, Maruyama D, Saito K, Toda A. 2001 A high-speed atomic force
953 microscope for studying biological macromolecules. *Proc. Natl Acad. Sci. USA* **98**, 12468–
954 12472. (doi:10.1073/pnas.211400898)
- 955 38. Ando T, Uchihashi T, Kodera N, Yamamoto D, Miyagi A, Taniguchi M, Yamashita
956 H. 2008 High-speed AFM and nano-visualization of biomolecular processes.
957 *Pflugers Archiv-Eur. J. Physiol.* **456**, 211–225. (doi:10.1007/s00424-007-0406-0)
- 958 39. Ando T. 2012 High-speed atomic force microscopy coming of age. *Nanotechnology* **23**, 062001.
959 (doi:10.1088/0957-4484/23/6/062001)

- 955 40. Hobbs JK, Vasilev C, Humphris ADL. 2006 VideoAFM—a new tool for high speed surface
956 analysis. *Analyst* **131**, 251–256. (doi:10.1039/B511330J)
- 957 41. Humphris ADL, Miles MJ, Hobbs JK. 2005 A mechanical microscope: high-speed atomic
958 force microscopy. *Appl. Phys. Lett.* **86**, 034106. (doi:10.1063/1.1855407)
- 959 42. Toshio A, Takayuki U, Noriyuki K. 2012 High-speed atomic force microscopy. *Japanese*
960 *J. Appl. Phys.* **51**, A02
- 961 43. Rico F, Gonzalez L, Casuso I, Puig-Vidal M, Scheuring S. 2013 High-speed force spectroscopy
962 unfolds titin at the velocity of molecular dynamics simulations. *Science* **342**, 741–743.
963 (doi:10.1126/science.1239764)
- 964 44. Rico F, Russek A, González L, Grubmüller H, Scheuring S. 2019 Heterogeneous and
965 rate-dependent streptavidin–biotin unbinding revealed by high-speed force spectroscopy
966 and atomistic simulations. *Proc. Natl Acad. Sci. USA* **116**, 6594–6601. (doi:10.1073/
967 pnas.1816909116)
- 968 45. Rigato A, Miyagi A, Scheuring S, Rico F. 2017 High-frequency microrheology reveals
969 cytoskeleton dynamics in living cells. *Nat. Phys.* **13**, 771–775.
- 970 46. Dong M, Sahin O. 2011 A nanomechanical interface to rapid single-molecule interactions.
971 *Nat. Commun.* **2**, 247. (doi:10.1038/ncomms1246)
- 972 47. Edwards DT, Perkins TT. 2016 Optimizing force spectroscopy by modifying commercial
973 cantilevers: improved stability, precision, and temporal resolution. *J. Struct. Biol.* **197**, 13–25.
- 974 48. Colom A, Casuso I, Rico F, Scheuring S. 2013 A hybrid high-speed atomic force-optical
975 microscope for visualizing single membrane proteins on eukaryotic cells. *Nat. Commun.* **4**,
976 2155. (doi:10.1038/ncomms3155)
- 977 49. Fukuda S, Uchihashi T, Iino R, Okazaki Y, Yoshida M, Igarashi K, Ando T. 2013 High-speed
978 atomic force microscope combined with single-molecule fluorescence microscope. *Rev. Sci.*
979 *Instrum.* **84**, 073706. (doi:10.1063/1.4813280)
- 980 50. Dufrene YF, Martinez-Martin D, Medalsy I, Alsteens D, Muller DJ. 2013 Multiparametric
981 imaging of biological systems by force-distance curve-based AFM. *Nat. Meth.* **10**, 847–854.
982 (doi:10.1038/nmeth.2602)
- 983 51. Hecht FM, Rheinlaender J, Schierbaum N, Goldmann WH, Fabry B, Schaffer TE. 2015
984 Imaging viscoelastic properties of live cells by AFM: power-law rheology on the nanoscale.
985 *Soft Matter* **11**, 4584–4591. (doi:10.1039/c4sm02718c)
- 986 52. Kim D, Sahin O. 2015 Imaging and three-dimensional reconstruction of chemical
987 groups inside a protein complex using atomic force microscopy. *Nat. Nano.* **10**, 264–269.
988 (doi:10.1038/nnano.2014.335)
- 989 53. Mandriota N, Friedsam C, Jones-Molina JA, Tatem KV, Ingber DE, Sahin O. 2019 Cellular
990 nanoscale stiffness patterns governed by intracellular forces. *Nat. Mater.* **18**, 1071–1077.
991 (doi:10.1038/s41563-019-0391-7)
- 992 54. Bangham AD, Pethica BA, Seaman GVF. 1958 The charged groups at the interface of some
993 blood cells. *Biochem. J.* **69**, 12–19. (doi:10.1042/bj0690012)
- 994 55. Singer SJ, Nicolson GL. 1972 Fluid mosaic model of structure of cell-membranes. *Science* **175**,
995 720–731. (doi:10.1126/science.175.4023.720)
- 996 56. Simons K, Ikonen E. 1997 Functional rafts in cell membranes. *Nature* **387**, 569–572.
997 (doi:10.1038/42408)
- 998 57. Goñi FM. 2019 ‘Rafts’: A nickname for putative transient nanodomains. *Chem. Phys. Lipids.*
999 **218**, 34–39. (doi:10.1016/j.chemphyslip.2018.11.006)
- 1000 58. Giocondi MC, Le Grimellec C. 2004 Temperature dependence of the surface topography
1001 in dimyristoylphosphatidylcholine/distearoylphosphatidylcholine multibilayers. *Biophys.*
1002 *J.* **86**, 2218–2230. (doi:10.1016/S0006-3495(04)74280-0)
- 1003 59. Takahashi H, Miyagi A, Redondo-Morata L, Scheuring S. 2016 Temperature-controlled
1004 high-speed AFM: real-time observation of ripple phase transitions. *Small* **12**, 6106–6113.
1005 (doi:10.1002/smll.201601549)
- 1006  Mandelbrot BB. In press. ~~The Fractal Geometry of Nature.~~
- 1007 61. Smith TG, Lange GD, Marks WB. 1996 Fractal methods and results in cellular
morphology - dimensions, lacunarity and multifractals. *J. Neurosci. Methods.* **69**, 123–136.
(doi:10.1016/S0165-0270(96)00080-5)
62. West GB, Brown JH, Enquist BJ. 1997 A general model for the origin of allometric scaling
laws in biology. *Science* **276**, 122–126. (doi:10.1126/science.276.5309.122)

- 1008 63. Weigel AV, Simon B, Tamkun MM, Krapf D. 2011 Ergodic and nonergodic processes coexist
1009 in the plasma membrane as observed by single-molecule tracking. *Proc. Natl Acad. Sci. USA*
1010 **108**, 6438–6443. (doi:10.1073/pnas.1016325108)
- 1011 64. Malchus N, Weiss M. 2010 Elucidating anomalous protein diffusion in living cells
1012 with fluorescence correlation spectroscopy-facts and pitfalls. *J. Fluoresc.* **20**, 19–26.
1013 (doi:10.1007/s10895-009-0517-4)
- 1014 65. Havlin S, Ben-Avraham D. 1987 Diffusion in disordered media. *Adv. Phys.* **36**, 695–798.
1015 (doi:10.1080/00018738700101072)
- 1016 66. Tremmel IG, Weis E, Farquhar GD. 2005 The influence of protein-protein interactions
1017 on the organization of proteins within thylakoid membranes. *Biophys. J.* **88**, 2650–2660.
1018 (doi:10.1529/biophysj.104.045666)
- 1019 67. Casuso I, Khao J, Chami M, Paul-Gilloteaux P, Husain M, Duneau J-P, Stahlberg H, Sturgis
1020 JN, Scheuring S. 2012 Characterization of the motion of membrane proteins using high-speed
1021 atomic force microscopy. *Nat. Nanotechnol.* **7**, 525–529. (doi:10.1038/nnano.2012.109)
- 1022 68. ~~Feder Jens. In press. Fractals~~ 
- 1023 69. Witten TA, Sander LM. 1981  Diffusion-limited aggregation, a kinetic critical phenomenon.
1024 *Phys. Rev. Lett.* **47**, 1400–1403. (doi:10.1103/PhysRevLett.47.1400)
- 1025 70. Spector J, Zakharov S, Lill Y, Sharma O, Cramer WA, Ritchie K. 2010 Mobility of BtuB and
1026 OmpF in the Escherichia coli outer membrane: implications for dynamic formation of a
1027 translocon complex. *Biophys. J.* **99**, 3880–3886. (doi:10.1016/j.bpj.2010.10.029)
- 1028 71. ~~In press. Fractals in Molecular Biophysics~~ ~~Ar: T. Gregory Dewey~~ ~~Ar: 9780195084474.~~
1029 ~~See [https://www.bookdepository.com/Fractals-Molecular-Biophysics-T-Gregory-Dewey/](https://www.bookdepository.com/Fractals-Molecular-Biophysics-T-Gregory-Dewey/9780195084474)~~
1030 ~~9780195084474 (accessed 30 April 2020).~~
- 1031 72. Duplantier B, Halsey TC, Rivasseau V. 2011 *Glasses and grains: poincaré seminar 2009*. Berlin,
1032 Germany: Springer Science & Business Media.
- 1033 73. Munguira I, Casuso I, Takahashi H, Rico F, Miyagi A, Chami M, Scheuring S. 2016
1034 Glasslike membrane protein diffusion in a crowded membrane. *Acs Nano* **10**, 2584–2590.
1035 (doi:10.1021/acsnano.5b07595)
- 1036 74. Yamaji-Hasegawa A, Hullin-Matsuda F, Greimel P, Kobayashi T. 2016 Pore-forming
1037 toxins: properties, diversity, and uses as tools to image sphingomyelin and ceramide
1038 phosphoethanolamine. *Biochim. et Biophys. Acta - Biomembr.* **1858**, 576–592. (doi:10.1016/j.
1039 bbmem.2015.10.012)
- 1040 75. Yamaji-Hasegawa A *et al.* 2003 Oligomerization and pore formation of a sphingomyelin-
1041 specific toxin, lysenin. *J. Biol. Chem.* **278**, 22 762–22 770. (doi:10.1074/jbc.M213209200)
- 1042 76. Goiko M, de Bruyn JR, Heit B. 2018 Membrane diffusion occurs by continuous-
1043 time random walk sustained by vesicular trafficking. *Biophys. J.* **114**, 2887–2899.
1044 (doi:10.1016/j.bpj.2018.04.024)
- 1045 77. Pastore R, Coniglio A, Ciamarra MP. 2015 Dynamic phase coexistence in glass-forming
1046 liquids. *Sci. Rep.* **5**, 1–10. (doi:10.1038/srep11770)
- 1047 78. Chiaruttini N, Roux A. 2017 Dynamic and elastic shape transitions in curved ESCRT-III
1048 filaments. *Curr. Opin Cell Biol.* **47**, 126–135. (doi:10.1016/j.ceb.2017.07.002)
- 1049 79. Chiaruttini N, Redondo-Morata L, Colom A, Humbert F, Lenz M, Scheuring S, Roux A. 2015
1050 Relaxation of loaded ESCRT-III spiral springs drives membrane deformation. *Cell* **163**, 866–
1051 879. (doi:10.1016/j.cell.2015.10.017)
- 1052 80. Mierzwa BE *et al.* 2017 Dynamic subunit turnover in ESCRT-III assemblies is regulated
1053 by Vps4 to mediate membrane remodelling during cytokinesis. *Nat. Cell Biol.* **19**, 787–798.
1054 (doi:10.1038/ncb3559)
- 1055 81. Colom A, Redondo-Morata L, Chiaruttini N, Roux A, Scheuring S. 2017 Dynamic remodeling
1056 of the dynamin helix during membrane constriction. *Proc. Natl Acad. Sci. USA* **114**, 5449–5454.
1057 (doi:10.1073/pnas.1619578114)
- 1058 82. Takeda T *et al.* 2018 Dynamic clustering of dynamin-amphiphysin helices regulates
1059 membrane constriction and fission coupled with GTP hydrolysis. *eLife* **7**, e30246.
1060 (doi:10.7554/eLife.30246)
- 1061 83. Kodera N, Yamamoto D, Ishikawa R, Ando T. 2010 Video imaging of walking myosin V by
1062 high-speed atomic force microscopy. *Nature* **468**, 72–76. (doi:10.1038/nature09450)
- 1063 84. Uchihashi T, Iino R, Ando T, Noji H. 2011 High-speed atomic force microscopy reveals rotary
1064 catalysis of rotorless F1-ATPase. *Science* **333**, 755–758. (doi:10.1126/science.1205510)

- 1061 85. Casuso I, Sens P, Rico F, Scheuring S. 2010 Experimental evidence for membrane-mediated
1062 protein-protein interaction. *Biophys. J.* **99**, L47–L49. (doi:10.1016/j.bpj.2010.07.028)
- 1063 86. Buzhynsky N, Sens P, Prima V, Sturgis JN, Scheuring S. 2007 Rows of ATP
1064 synthase dimers in native mitochondrial inner membranes. *Biophys. J.* **93**, 2870–2876.
1065 (doi:10.1529/biophysj.107.109728)
- 1066 87. Crampton N, Yokokawa M, Dryden DTF, Edwardson JM, Rao DN, Takeyasu K, Yoshimura
1067 SH, Henderson RM. 2007 Fast-scan atomic force microscopy reveals that the type III
1068 restriction enzyme EcoP15I is capable of DNA translocation and looping. *Proc. Natl Acad.
1069 Sci. USA* **104**, 12755–12760. (doi:10.1073/pnas.0700483104)
- 1070 88. Levinthal C. 1968 Are there pathways for protein folding? *Extrait du J. de Chimie Phys.* **65**, 44.
1071 (doi:10.1051/jcp/1968650044)
- 1072 89. Frauenfelder H, Sligar SG, Wolynes PG. 1991 The energy landscapes and motions of proteins.
1073 *Science* **254**, 1598–1603. (doi:10.1126/science.1749933)
- 1074 90. Ansari A, Berendzen J, Bowne SF, Frauenfelder H, Iben IET, Sauke TB, Shyamsunder E,
1075 Young RD. 1985 Protein states and protein quakes. *Proc. Natl Acad. Sci. USA* **82**, 5000–5004.
1076 (doi:10.1073/pnas.82.15.5000)
- 1077 91. Bryngelson JD, Onuchic JN, Socci ND, Wolynes PG. 1995 Funnels, pathways, and the
1078 energy landscape of protein folding: a synthesis. *Proteins: Struct. Funct. Bioinf.* **21**, 167–195.
1079 (doi:10.1002/prot.340210302)
- 1080 92. Schramm A, Bignon C, Brocca S, Grandori R, Santambrogio C, Longhi S. 2019 An arsenal
1081 of methods for the experimental characterization of intrinsically disordered proteins –
1082 how to choose and combine them? *Arch. Biochem. Biophys.* **676**, 108055. (doi:10.1016/j.
1083 abb.2019.07.020)
- 1084 93. Ando T, Kodera N. 2012 Visualization of mobility by atomic force microscopy. In *Intrinsically
1085 disordered protein analysis*, pp. 57–69. Berlin, Germany: Springer.
- 1086 94. Miyagi A, Tsunaka Y, Uchihashi T, Mayanagi K, Hirose S, Morikawa K, Ando T. 2008
1087 Visualization of intrinsically disordered regions of proteins by high-speed atomic force
1088 microscopy. *Chemphyschem* **9**, 1859–1866. (doi:10.1002/cphc.200800210)
- 1089 95. Hashimoto M, Kodera N, Tsunaka Y, Oda M, Tanimoto M, Ando T, Morikawa K, Tate S. 2013
1090 Phosphorylation-coupled intramolecular dynamics of unstructured regions in chromatin
1091 remodeler FACT. *Biophys. J.* **104**, 2222–2234. (doi:10.1016/j.bpj.2013.04.007)
- 1092 96. Hughes ML, Dougan L. 2016 The physics of pulling polypeptides: a review of single molecule
1093 force spectroscopy using the AFM to study protein unfolding. *Rep. Prog. Phys.* **79**, 076601.
1094 (doi:10.1088/0034-4885/79/7/076601)
- 1095 97. Carrion-Vazquez M, Oberhauser AF, Fowler SB, Marszalek PE, Broedel SE, Clarke J,
1096 Fernandez JM. 1999 Mechanical and chemical unfolding of a single protein: a comparison.
1097 *Proc. Natl Acad. Sci. USA* **96**, 3694–3699. (doi:10.1073/pnas.96.7.3694)
- 1098 98. Li H, Oberhauser AF, Redick SD, Carrion-Vazquez M, Erickson HP, Fernandez JM. 2001
1099 Multiple conformations of PEVK proteins detected by single-molecule techniques. *Proc. Natl
1100 Acad. Sci. USA* **98**, 10682–10686. (doi:10.1073/pnas.191189098)
- 1101 99. Ando T, Uchihashi T, Scheuring S. 2014 Filming biomolecular processes by high-speed
1102 atomic force microscopy. *Chem. Rev.* **114**, 3120–3188. (doi:10.1021/cr4003837)
- 1103 100. Matsushita K, Kikuchi M. 2013 Frustration-induced protein intrinsic disorder. *J. Chem. Phys.*
1104 **138**, 105101. (doi:10.1063/1.4794781)
- 1105 101. Kellermayer MSZ, Smith SB, Granzier HL, Bustamante C. 1997 Folding-unfolding transitions
1106 in single titin molecules characterized with laser tweezers. *Science* **276**, 1112–1116.
1107 (doi:10.1126/science.276.5315.1112)
- 1108 102. Valotteau C, Sumbul F, Rico F. 2019 High-speed force spectroscopy: microsecond
1109 force measurements using ultrashort cantilevers. *Biophys. Rev.* **11**, 689–699.
1110 (doi:10.1007/s12551-019-00585-4)
- 1111 103. Lee EH, Hsin J, Sotomayor M, Comellas G, Schulten K. 2009 Discovery through the
1112 computational microscope. *Structure* **17**, 1295–1306. (doi:10.1016/j.str.2009.09.001)
- 1113 104. Jacobson DR, Uyetake L, Perkins TT. 2020 Membrane-protein unfolding intermediates
detected with enhanced precision using a zigzag force ramp. *Biophys. J.* **118**, 667–675.
(doi:10.1016/j.bpj.2019.12.003)
105. Evans E, Ritchie K. 1997 Dynamic strength of molecular adhesion bonds. *Biophys. J.* **72**, 1541–
1555. (doi:10.1016/S0006-3495(97)78802-7)

- 1114 106. Lu H, Isralewitz B, Krammer A, Vogel V, Schulten K. 1998 Unfolding of titin
1115 immunoglobulin domains by steered molecular dynamics simulation. *Biophys. J.* **75**, 662–671.
1116 (doi:10.1016/S0006-3495(98)77556-3)
- 1117 107. Takahashi H, Rico F, Chipot C, Scheuring S. 2018 α -Helix unwinding as force buffer in
1118 spectrins. *ACS Nano* **12**, 2719–2727. (doi:10.1021/acsnano.7b08973)
- 1119 108. Sumbul F, Marchesi A, Rico F. 2018 History, rare, and multiple events of mechanical
1120 unfolding of repeat proteins. *J. Chem. Phys.* **148**, 123335. (doi:10.1063/1.5013259)
- 1121 109. Franz F, Daday C, Gräter F. 2020 Advances in molecular simulations of protein mechanical
1122 properties and function. *Curr. Opin Struct. Biol.* **61**, 132–138. (doi:10.1016/j.sbi.2019.12.015)
- 1123 110. Marszalek PE, Lu H, Li H, Carrion-Vazquez M, Oberhauser AF, Schulten K, Fernandez
1124 JM. 1999 Mechanical unfolding intermediates in titin modules. *Nature* **402**, 100–103.
1125 (doi:10.1038/47083)
- 1126 111. Lenne P-F, Raae AJ, Altmann SM, Saraste M, Hörber JKH. 2000 States and transitions
1127 during forced unfolding of a single spectrin repeat. *FEBS Lett.* **476**, 124–128.
1128 (doi:10.1016/S0014-5793(00)01704-X)
- 1129 112. Nunes JM, Hensen U, Ge L, Lipinsky M, Helenius J, Grubmüller H, Müller DJ. 2010
1130 A 'Force Buffer' protecting immunoglobulin titin. *Angew. Chem. Int. Ed.* **49**, 3528–3531.
1131 (doi:10.1002/anie.200906388)
- 1132 113. Oesterhelt F, Oesterhelt D, Pfeiffer M, Engel A, Gaub HE, Müller DJ. 2000 Unfolding
1133 pathways of individual bacteriorhodopsins. *Science* **288**, 143–146. (doi:10.1126/
1134 science.288.5463.143)
- 1135 114. Yu H, Siewny MGW, Edwards DT, Sanders AW, Perkins TT. 2017 Hidden dynamics
1136 in the unfolding of individual bacteriorhodopsin proteins. *Science* **355**, 945–950.
1137 (doi:10.1126/science.aah7124)
- 1138 115. Kappel C, Grubmüller H. 2011 Velocity-dependent mechanical unfolding of
1139 bacteriorhodopsin is governed by a dynamic interaction network. *Biophys. J.* **100**, 1109–1119.
1140 (doi:10.1016/j.bpj.2011.01.004)
- 1141 116. Izrailev S, Stepaniants S, Balsera M, Oono Y, Schulten K. 1997 Molecular dynamics
1142 study of unbinding of the avidin-biotin complex. *Biophys. J.* **72**, 1568–1581.
1143 (doi:10.1016/S0006-3495(97)78804-0)
- 1144 117. Grubmüller H, Heymann B, Tavan P. 1996 Ligand binding: molecular mechanics
1145 calculation of the streptavidin biotin rupture force. *Science* **271**, 997–999. (doi:10.1126/
1146 science.271.5251.997)
- 1147 118. Bell GI. 1978 Models for specific adhesion of cells to cells. *Science* **200**, 618–627.
1148 (doi:10.1126/science.347575)
- 1149 119. Hummer G, Szabo A. 2003 Kinetics from nonequilibrium single-molecule pulling
1150 experiments. *Biophys. J.* **85**, 5–15. (doi:10.1016/S0006-3495(03)74449-X)
- 1151 120. Bullerjahn JT, Sturm S, Kroy K. 2014 Theory of rapid force spectroscopy. *Nat. Commun.* **5**,
1152 Article number: 4463. (doi:10.1038/ncomms5463)
- 1153 121. Dudko OK, Hummer G, Szabo A. 2006 Intrinsic rates and activation free energies
1154 from single-molecule pulling experiments. *Phys. Rev. Lett.* **96**, 108101. (doi:10.1103/
1155 PhysRevLett.96.108101)
- 1156 122. Dudko OK, Hummer G, Szabo A. 2008 Theory, analysis, and interpretation of single-
1157 molecule force spectroscopy experiments. *Proc. Natl Acad. Sci. USA* **105**, 15755–15760.
1158 (doi:10.1073/pnas.0806085105)
- 1159 123. Friddle RW. 2008 Unified model of dynamic forced barrier crossing in single molecules. *Phys.*
1160 *Rev. Lett.* **100**, 138302. (doi:10.1103/PhysRevLett.100.138302)
- 1161 124. Lin H-J, Chen H-Y, Sheng Y-J, Tsao H-K. 2007 Bell's expression and the generalized
1162 Garg form for forced dissociation of a biomolecular complex. *Phys. Rev. Lett.* **98**, 088304.
1163 (doi:10.1103/PhysRevLett.98.088304)
- 1164 125. Hyeon C, Thirumalai D. 2012 Multiple barriers in forced rupture of protein complexes.
1165 *J. Chem. Phys.* **137**, 055103. (doi:10.1063/1.4739747)
- 1166 126. Merkel R, Nassoy P, Leung A, Ritchie K, Evans E. 1999 Energy landscapes of receptor-ligand
bonds explored with dynamic force spectroscopy. *Nature* **397**, 50–53. (doi:10.1038/16219)
127. Cossio P, Hummer G, Szabo A. 2016 Kinetic ductility and force-spike resistance
of proteins from single-molecule force spectroscopy. *Biophys. J.* **111**, 832–840.
(doi:10.1016/j.bpj.2016.05.054)

- 1167 128. Kroy K. 2017 The benefits of getting high. *Nat. Phys.* **13**, 728–729. (doi:10.1038/nphys4128)
- 1168 129. Friddle RW, Noy A, De Yoreo JJ. 2012 Interpreting the widespread nonlinear force
- 1169 spectra of intermolecular bonds. *Proc. Natl Acad. Sci. USA* **109**, 13 573–13 578. (doi:10.1073/
- 1170 [pnas.1202946109](https://doi.org/10.1073/pnas.1202946109))
- 1171 130. Yamaoka H, Matsushita S, Shimada Y, Adachi T. 2012 Multiscale modeling and
- 1172 mechanics of filamentous actin cytoskeleton. *Biomech. Model. Mechanobiol.* **11**, 291–302.
- 1173 (doi:10.1007/s10237-011-0317-z)
- 1174 131. Allain PE *et al.* 2020 Optomechanical resonating probe for very high frequency sensing of
- 1175 atomic forces. *Nanoscale* **12**, 2939–2945. (doi:10.1039/C9NR09690F)
- 1176 132. Costescu BI, Sturm S, Gräter F. 2016 Dynamic disorder can explain non-exponential kinetics
- 1177 of fast protein mechanical unfolding. *J. Struct. Biol.* **197**, 43–49.
- 1178 133. Hinczewski M, Hyeon C, Thirumalai D. 2016 Directly measuring single-molecule
- 1179 heterogeneity using force spectroscopy. *Proc. Natl Acad. Sci. USA* **113**, E3852–E3861.
- 1180 (doi:10.1073/pnas.1518389113)
- 1181 134. Brujic J, Hermans RI, Walther KA, Fernandez JM. 2006 Single-molecule force spectroscopy
- 1182 reveals signatures of glassy dynamics in the energy landscape of ubiquitin. *Nat. Phys.* **2**,
- 1183 282–286. (doi:10.1038/nphys269)
- 1184
- 1185
- 1186
- 1187
- 1188
- 1189
- 1190
- 1191
- 1192
- 1193
- 1194
- 1195
- 1196
- 1197
- 1198
- 1199
- 1200
- 1201
- 1202
- 1203
- 1204
- 1205
- 1206
- 1207
- 1208
- 1209
- 1210
- 1211
- 1212
- 1213
- 1214
- 1215
- 1216
- 1217
- 1218
- 1219